DEVELOPMENT STATUS OF A THIN LENS MODEL FOR FRIB ONLINE MODEL SERVICE*

G. Shen, Z. He#, FRIB, Michigan State University, East Lansing, 48864 USA

Abstract

FRIB (Facility for Rare Isotope Beams) is a heavy ion linac facility under construction, which has various specific features in its beam dynamics design to achieve the world highest beam power for heavy ion linacs. It is a challenge to develop an online model which covers all those specific features and satisfies the requirement for execution speed at the same time. An online model named TLM (Thin Lens Model) is under active development at FRIB to address its all major beam dynamics issues. This paper describes the latest status of TLM code, the infrastructure to integrate the TLM into FRIB beam commissioning environment.

INTRODUCTION

FRIB [1, 2] is a new project funded by DOE and MSU (Michigan State University), and under construction on the campus of MSU and will be a new national user facility for nuclear science. Its driver accelerator is designed to accelerate all stable ions to energies > 200 MeV/u with beam power on the target up to 400 kW. It consists of 2 ECR (Electron Cyclotron Resonance) ion sources, a low energy beam transport, a RFQ (Radio Frequency Quadrupole) linac, 3 Linac segments, 2 folding segments to confine the footprint and facilitate charge selection, and a beam delivery system to transport to the target. The beam is stripped to higher charge states in the first LS section (LS1).

TLM ONLINE MODEL

As mentioned in [3], an online model is under active development at FRIB to meet its needs. The emphasis of the development is put on the execution speed and coverage of FRIB specific needs. The FRIB lattice is designed with some specific features as summarized below:

- Solenoid focusing lattice;
- Non-axisymmetric field components at QWRs (Quarter Wave Resonators). The non-axisymmetric nature of QWR induces dipole and quadrupole components, which has significant contribution to FRIB beam dynamics;
- Multi-charge-state beam acceleration. FRIB is designed to accelerate up to five charge states simultaneously to achieve high beam intensity. It is a challenge to meet stringent beam-on-target requirements especially for multi-charge-state beams;
- Achromat arc sections between linac segments;
- Second order achromat with sextupole magnets.

To commission the beam effectively and efficiently, an online model named TLM (Thin Lens Model) is under active development at FRIB to address those issues. It currently supports optical elements including dipole magnet, quadrupole magnet, solenoid magnet, axisymmetric RF cavity and non-axisymmetric RF cavity, corrector magnet, stripper, electrostatic optical elements (dipole and quadrupole), and diagnostic devices.

RF Cavity

There are 2 major considerations about FRIB cavity modelling, which are 1) significant velocity change especially in low energy range, and 2) multipole field component effect caused by the non-axisymmetric geometry of its cavity.

A full implementation of FRIB RF cavity has been published in [4,5]. In short, because FRIB needs to accelerate up to 5 different beams simultaneously, traditional one gap approach, which has been widely used in many envelope-tracking codes, does not apply to FRIB, especially for its low-energy part. Therefore, TLM adopts field integration to track the reference particle, and two-gap model for transfer matrix calculation.

Solenoid

The FRIB adopts solenoid lattice instead of quadrupole lattice acting as the only focusing component for all four cryomodules. Solenoid focusing lattice introduces strong coupling effect between horizontal and vertical directions. A realistic solenoid has fringe effect, which has to be modeled properly.

With the rotating Larmor frame, the transfer matrix of solenoid can be decomposed into two commuting transfer matrix: one rotating and one constant focusing. The solenoid is treated as a constant focusing element when in the Larmor frame. Figure 1 shows an example of transverse design for oxygen lattice when using Larmor frame to simplify designing procedure.

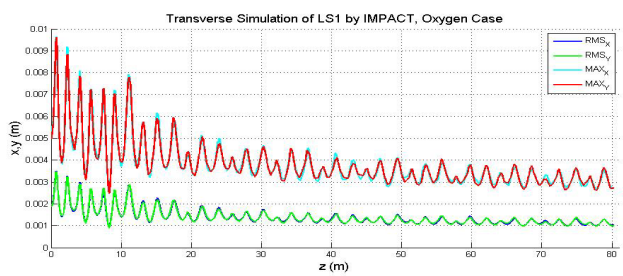

Figure 1: example of transverse design for oxygen lattice using Larmor frame and confirmation of beam envelope using IMPACT-Z [6].

There are two main effects of solenoid fringe field, one is decreasing of focusing strength, and another is decreas-

*Work supported by the U.S. Department of Energy Office of Science under Cooperative Agreement DE-SC0000661
#hez@frib.msu.edu

ISBN 978-3-95450-136-6

ing of rotating Larmor angle. Decrease of Larmor angle is proportional to field integration and is easy to calculate. We model the focusing reducing effect by adding two defocusing thin lens kick described as Eq. (1) [7].

$$M_{edge} = \begin{bmatrix} 1 & 0 & 0 & 0 & 0 & 0 \\ -\Phi & 1 & 0 & 0 & 0 & 0 \\ 0 & 0 & 1 & 0 & 0 & 0 \\ 0 & 0 & -\Phi & 1 & 0 & 0 \\ 0 & 0 & 0 & 0 & 1 & 0 \\ 0 & 0 & 0 & 0 & 0 & 1 \end{bmatrix} \quad (1)$$

Where $\Phi = \frac{-g^2 a}{2}$, g is focusing strength proportional to B and a is aperture size. An estimated solenoid fringe effect using Eq. (1) shows that adding fringe effect results in significant envelope blow up as illustrated in Fig. 2:

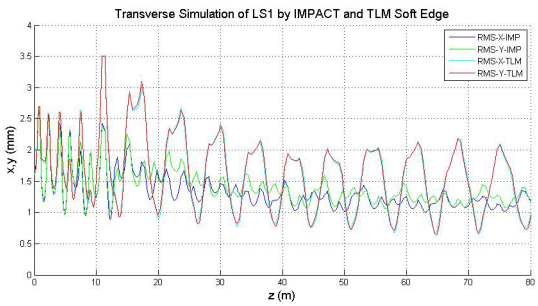

Figure 2: Horizontal and vertical envelope with (blue and green) and without (cyan and red) solenoid fringe.

Electrostatic Element

The electrostatic optical elements include dipole and quadrupole component and are used in FRIB front-end section. The transfer matrix of an electrostatic quadrupole is basically the same as magnetic quadrupole after changing definition of focusing strength into Eq. (2) [8]:

$$k^2 = \frac{q}{\beta^2 \gamma E_s} \frac{V_0}{R^2} \quad (2)$$

Where V_0 is the voltage of electrode and R is the radius. The transfer matrix for a hardedge spherical electrostatic bend is Eq. (3) [8]:

$$\begin{bmatrix} x_2 \\ x_2' \\ \delta_K \\ \delta_m \end{bmatrix} = \begin{bmatrix} c_x & s_x & d_x N_k & d_x N_m \\ -s_x k_x^2 & c_x & (s_x/\rho_0) N_k & (s_x/\rho_0) N_m \\ 0 & 0 & 1 & 0 \\ 0 & 0 & 0 & 1 \end{bmatrix} \begin{bmatrix} x_1 \\ x_1' \\ \delta_K \\ \delta_m \end{bmatrix}$$

$$\begin{bmatrix} y_2 \\ y_2' \end{bmatrix} = \begin{bmatrix} c_y & s_y \\ -s_y k_y^2 & c_y \end{bmatrix} \begin{bmatrix} y_1 \\ y_1' \end{bmatrix} \quad (3)$$

Where $c_x = \cos(k_x L)$, $s_x = \sin(k_x L)/k_x$, $d_x = \frac{1-\cos(k_x L)}{\rho_0 k_x^2}$, $c_y = \cos(k_y L)$, $s_y = \frac{\sin(k_y L)}{k_y}$, $N_K = \frac{(1+2\eta_0)^2+1}{2(1+\eta_0)(1+2\eta_0)}$, $N_m = \frac{(1+2\eta_0)-1}{2(1+\eta_0)(1+2\eta_0)}$, $\eta_0 = \frac{m-m_0}{2m_0}$, $\delta_k = \frac{K}{K_0} - 1$, $\delta_m = \frac{(m/z)}{(m/z_0)} - 1$, $k_x^2 \rho_0^2 = 1 - n_1 + \frac{1}{(1+2\eta_0)^2}$, $k_y^2 \rho_0^2 = n_1$, for spherical electrostatic bend, n_1=1, ρ_0 is bending radius, m is particle mass, m_0 is static mass, K is particle kinetic energy, K_0 is reference particle kinetic energy, z is particle charge state, z_0 is reference particle charge state.

Stripper

There exists three effects needed to take into consideration to model a stripper, which are 1) change in charge state, 2) energy straggling, and 3) blow up in phase space respectively.

Charge states distribution after stripping is calculated by Baron's formula [9]:

$$\frac{\bar{Q}}{Z} = 1 - exp\left(-83.275 \frac{\beta}{Z^{0.447}}\right)$$
$$Q_{ave} = \bar{Q}\left(1 - exp(-12.905 + 0.2124Z - 0.00122Z^2)\right)$$
$$d = \sqrt{\bar{Q}(0.07535 + 0.19Y - 0.2654Y^2)}, Y = \bar{Q}/Z \quad (4)$$

Q_{ave} is the average output charge state and d is standard deviation. Gaussian distribution of output charge state is assumed. Baron's formula can be benchmarked with NSCL data, for Uranium Z=92, E_k=9.92MeV/u (Fig. 3):

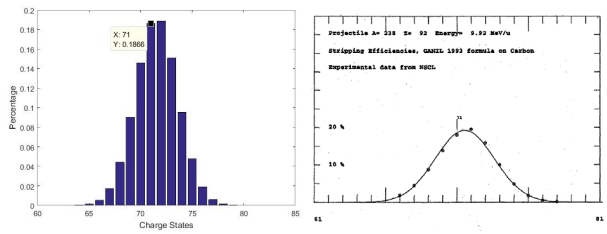

Figure 3: charge state distribution calculated using Baron's formula and benchmark with NSCL data.

Modelling of energy straggling effect and phase-space blow-up effect starts with SRIM [10] Monte-Carlo simulation. SRIM is able to calculate particle energy and momentum after particles injected into a certain stripper material. Then, an empirical formula in Eq. (5) is adopted to fit the results and the obtained parameters are used for stripper modelling:

$$f(\theta, E) = (\theta/\theta_N) \cdot e^{-\left(\frac{\theta}{\theta_2}\right)^u} \cdot e^{-\frac{1}{2}\left[\frac{(E-E_0)}{E_1}\right]^2} \quad (5)$$

The energy straggling effect can be get from parameter E_0, and the envelope blow up effect can be estimated using Eq. (6):

$$\sigma_h = \sqrt{\sigma_f^2 + \sigma_g^2} \quad (6)$$

σ_f is the standard deviation of original beam; σ_g is an extra standard deviation added solely with stripper; σ_h is the resulting standard deviation. The model is then benchmarked with a particle tracking code IMPACT-Z, results are shown in Fig. 4.

Multi-charge State

FRIB is simultaneously accelerating multiple charge states in order to enhance the beam current. Instead of conventional particle tracking method, TLM is utilizing a divide-and conquer three-step-scheme to track multi-charge state beam.

- Step 1: Machine initialization by reference charge state: An ideal particle with a center charge state is used to initialize the whole machine, mainly the cavity phase;

ISBN 978-3-95450-136-6

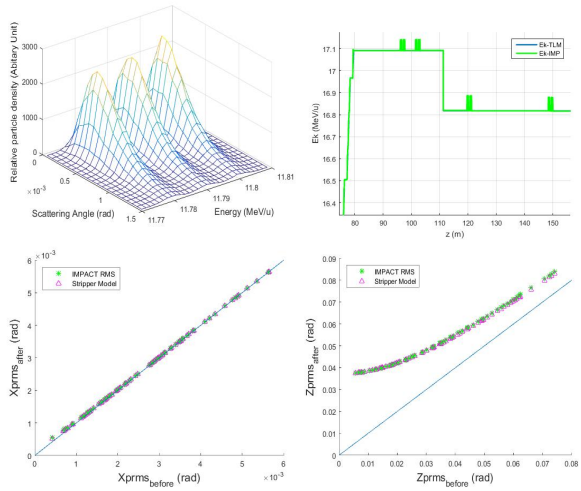

Figure 4: (a) Energy and angle distribution simulated by SRIM (b) Energy straggling effect benchmarked with IMPACT (c) Transverse momentum rms blow up and benchmark with IMPACT (d) Longitudinal momentum rms blow up and benchmark with IMPACT-Z.

- Step 2: Reference orbit initialization of the reference particle for each charge states: single particle tracking is used for a reference particle for each charge states and the result is recorded for reference
- Step3: Envelope tracking for each charge state: transfer matrix is adjusted according to different charge states and its different reference orbit.

The method and benchmark has been thoroughly discussed in [11].

BENCHMARK

The result of TLM simulation has been benchmarked with some well-recognized codes to crosscheck its result. We choose our lattice design codes, which is DIMAD for our front-end and IMPACT-Z for main linac, to verify the simulation results.

For the main linac, the results are compared including both transverse plane and longitudinal plane within acceptable error range. Two typical examples are as shown in Fig. 5, which are for central beam orbit for LS1 segment, and energy for LS1 and FS1 segments. The accumulated error is within 2% for orbit, and 0.005% for energy.

For the front-end, the results are benchmarked against DIMAD [12] code, and results for both horizontal and vertical envelope are shown in Fig. 6. The accumulated RMS error has been achieved within 0.01%.

CONCLUSION

An online model is under active development at FRIB to support FRIB specific requirements. Implementation of major functions and optical elements are finished and the simulation results are benchmarked against various well-recognized simulation such as IMPACT-Z and DIMAD, and a good agreement has achieved within acceptable error range. The online model has been now integrated

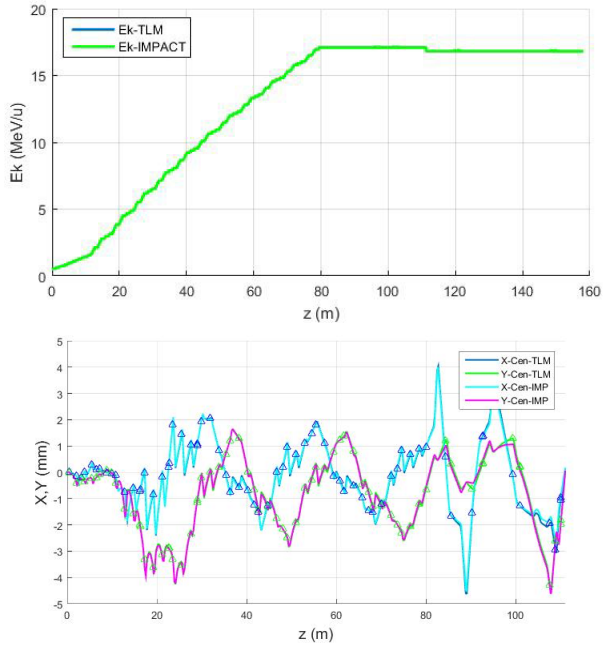

Figure 5: Benchmark results against IMPACT-Z of central beam trajectory (top) for LS1 segment, and beam energy for LS1 and FS1 segments (bottom).

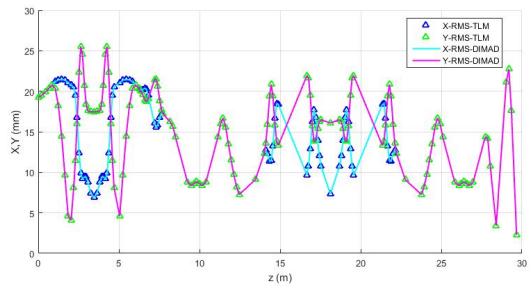

Figure 6: Benchmark results against DIMAD of X/Y envelope for FRIB FE using the lattice of Artemis IS.

into FRIB commissioning software framework, and the development of physics application has been started with the support of the online model.

ACKNOWLEDGMENT

The authors would thank our FRIB colleagues, especially M. Ikegami, S. Lund, E. Pozdeyev, J. Wei, Y. Yamazaki, Q. Zhao, Y. Zhang, for their helpful discussions and suggestions. They want to thank D. Bailey and Z. Zheng for providing the field maps for RF cavity and for electrostatic bend. They also would like to thank Prof M. Berz at MSU and his group for sharing the COSY code.

REFERENCES

[1] http://www.frib.msu.edu
[2] J. Wei et al, “FRIB Accelerator: Design and Construction Status”, MOM1I02, proceedings of HIAT’15, Yokohama, Japan (2015)

ISBN 978-3-95450-136-6

[3] M. Ikegami, G. Shen, “Development Plan for Physics Application Software for FRIB Driver Linac”, MOPWI023, proceedings of IPAC15, VA, US (2015)

[4] Z. He et al., “An Analytical Cavity Model for Fast Linac-Beam Tuning”, TUPB058, proceedings of LINAC2012, Tel-Aviv, Israel (2012)

[5] Z. He et al., “Beam Dynamic Influence From Quadrupole Components in FRIB Quarter Wave Resonators”, MOPAB35, proceedings of HB2014, East-Lansing, MI, USA (2014)

[6] J. Qiang et al., Impact. In Proceedings of the 1999 ACM/IEEE conference on Supercomputing, page 55. ACM, 1999.

[7] Aslaninejad, M. et al "Solenoid fringe fields effects for the Neutrino Factory linac-MADX investigation." IPAC 10 (2010): 3963.

[8] Wollnik, Hermann. Optics of charged particles. Elsevier, 2012.

[9] E. Baron, G ANIL Report 79R/146/TF14

[10] Ziegler, James F., Matthias D. Ziegler, and Jochen P. Biersack. SRIM. Cadence Design Systems, 2008.

[11] Z. He et al., "Linear envelope model for multicharge state linac." Physical Review Special Topics-Accelerators and Beams 17, no. 3 (2014): 034001.

[12] R. Servranckx, K. Brown, L. Schachinger, and D. Douglas, “User’s Guide to the Program DIMAD”, SLAC Report 285, UC-28, May 1985.

ISBN 978-3-95450-136-6